Dysregulated copper transport in multiple sclerosis may cause demyelination via astrocytes

Emanuela Colombo[a], Daniela Triolo[a], Claudia Bassani[a], Francesco Bedogni[b,1], Marco Di Dario[a], Giorgia Dina[a], Evelien Fredrickx[a], Isabella Fermo[c], Vittorio Martinelli[a], Jia Newcombe[d], Carla Taveggia[a], Angelo Quattrini[a], Giancarlo Comi[a], and Cinthia Farina[a,2]

[a]Division of Neuroscience, Institute of Experimental Neurology, Istituto di Ricovero e Cura a Carattere Scientifico (IRCCS) San Raffaele Scientific Institute, 20132, Milan, Italy; [b]San Raffaele Rett Research Centre, Istituto di Ricovero e Cura a Carattere Scientifico (IRCCS) San Raffaele Scientific Institute, 20132, Milan, Italy; [c]Division of Immunology, Transplantation, and Infectious Diseases, Istituto di Ricovero e Cura a Carattere Scientifico (IRCCS) San Raffaele Scientific Institute, 20132, Milan, Italy; and [d]NeuroResource, Department of Neuroinflammation, UCL Queen Square Institute of Neurology, WC1N 1PJ, London, UK

Edited by Lawrence Steinman, Stanford University School of Medicine, Stanford, CA, and approved May 21, 2021 (received for review December 18, 2020)

Demyelination is a key pathogenic feature of multiple sclerosis (MS). Here, we evaluated the astrocyte contribution to myelin loss and focused on the neurotrophin receptor TrkB, whose up-regulation on the astrocyte finely demarcated chronic demyelinated areas in MS and was paralleled by neurotrophin loss. Mice lacking astrocyte TrkB were resistant to demyelination induced by autoimmune or toxic insults, demonstrating that TrkB signaling in astrocytes fostered oligodendrocyte damage. In vitro and ex vivo approaches highlighted that astrocyte TrkB supported scar formation and glia proliferation even in the absence of neurotrophin binding, indicating TrkB transactivation in response to inflammatory or toxic mediators. Notably, our neuropathological studies demonstrated copper dysregulation in MS and model lesions and TrkB-dependent expression of copper transporter (CTR1) on glia cells during neuroinflammation. In vitro experiments evidenced that TrkB was critical for the generation of glial intracellular calcium flux and CTR1 up-regulation induced by stimuli distinct from neurotrophins. These events led to copper uptake and release by the astrocyte, and in turn resulted in oligodendrocyte loss. Collectively, these data demonstrate a pathogenic demyelination mechanism via the astrocyte release of copper and open up the possibility of restoring copper homeostasis in the white matter as a therapeutic target in MS.

astrocyte | copper | demyelination | multiple sclerosis | TrkB

Astrocytes are the largest population of glial cells in the central nervous system (CNS) and are essential for brain homeostasis as they provide metabolites and growth factors to neurons, support synapse formation and plasticity, contribute to the blood brain barrier (BBB) structure and function, and support myelination (1, 2). Following CNS injury they undergo molecular and functional changes, which foster acquisition of an inflammatory phenotype, migration toward damaged areas, and proliferation and organization into the scar (1). These events are fundamental for tissue repair but bear the potential of hindering damage resolution if dysregulated under pathologic conditions (3). Multiple sclerosis (MS) is a chronic inflammatory disorder of the CNS characterized by demyelination, inflammation, and neuroaxonal damage (4). While active MS plaques are rich in infiltrating immune cells, activated microglia and macrophages throughout the partially demyelinated astrogliotic lesion, chronic inactive MS plaques lack T cell infiltration and are fully demyelinated sites with sharply demarcated borders, very low myeloid cell numbers, severe axonal injury, and dense astrocytic scars (5, 6). In vivo studies with transgenic animals have highlighted detrimental vs. protective signaling perturbations in astrocytes during CNS neuroinflammation (3), but the precise causal mechanisms linking the target to distinct neuropathological outcomes (e.g., immune cell infiltration, neurodegeneration, or demyelination) remain mostly ill-defined. For example, the neurotrophin receptor TrkB is up-regulated on astrocytes in chronic inactive MS lesions, where it promotes neurodegeneration via glial production of nitric oxide (NO) (7); however no information is available about the impact of TrkB signaling in astrocytes during demyelination. Further, astrocytes are concomitantly exposed to diverse stimuli within the scar (3, 8) and can activate an intricate network of intracellular events, with a net result remaining difficult to predict until relevant molecular and functional checkpoints are identified.

Here, we describe a demyelination mechanism resulting from astrocyte-dependent copper redistribution in the white matter of MS patients and experimental models of MS. The relevant molecular checkpoint in astrocytes is TrkB, which can operate downstream of inflammatory or toxic insults, even in the absence of neurotrophin binding, and trigger astrocytosis and copper uptake and release following injury.

Results

TrkB Ligands Are Not Expressed in Chronic MS White Matter Lesions. As astrocytes can up-regulate TrkB in MS lesions and trigger neurodegeneration in response to neurotrophins (7), we searched for the expression of TrkB ligands in MS chronic inactive plaques where the fully demyelinated white matter (WM) is flanked by normal-appearing white matter (NAWM). In situ hybridization (ISH) combined with GFAP and/or MBP immunostainings on MS brain sections showed that BDNF mRNA was scarce in the

Significance

This study describes an astrocyte-dependent mechanism contributing to CNS demyelination. The key molecular and functional checkpoint is the neurotrophin receptor TrkB, whose ligands are absent in chronic demyelinated MS lesions. Here, we show that TrkB can be transactivated by inflammatory and toxic signals and is critical for the generation of glial calcium flux and the up-regulation of the copper transporter CTR1. This process enhances copper distribution by the astrocyte, thereby fostering myelin and oligodendrocyte loss.

Author contributions: E.C. and C.F. designed experiments; E.C., D.T., C.B., F.B., M.D.D., G.D., E.F., and I.F. performed research; V.M., J.N., C.T., A.Q., and G.C. contributed new reagents/analytic tools; E.C. and C.F. analyzed data; E.C. and C.F. wrote the paper; and C.F. designed and supervised the research.

The authors declare no competing interest.

This article is a PNAS Direct Submission.

See online for related content such as Commentaries.

[1]Present address: Neuroscience and Mental Health Research Institute, Division of Neuroscience, School of Biosciences, CF24 4HQ, Cardiff, UK.

[2]To whom correspondence may be addressed. Email: farina.cinthia@hsr.it.

This article contains supporting information online at https://www.pnas.org/lookup/suppl/doi:10.1073/pnas.2025804118/-/DCSupplemental.

Published June 28, 2021.

glial scar but abundant in the neighboring NAWM (Fig. 1 *A* and *B* and *SI Appendix*, Fig. S1 *A* and *B*).

Interestingly, TrkB and MBP staining patterns were mutually exclusive, as astrocyte TrkB finely demarcated demyelinated MBP-negative MS plaques (Fig. 1 *C–E* and *SI Appendix*, Fig. S1 *C* and *D*), suggesting a role for TrkB in demyelination in MS. Importantly, MS WM lesions displayed low BDNF and NT4 proteins, which were present at high levels in the NAWM (Fig. 1 *F* and *G* and *SI Appendix*, Fig. S1 *C*, *E*, and *F*), while another possible TrkB ligand, NT3, was scarcely expressed in these tissues (Fig. 1*H*).

Thus, although astrocytes may support oligodendrogliogenesis via BDNF (9) and BDNF may be delivered by immune cells infiltrating active MS lesions (10), chronic inactive demyelinated plaques showed blunted levels of TrkB ligands, suggesting that the robust TrkB signal operates in response to other stimuli during neuroinflammation.

TrkB Expression in Astrocytes Supports Demyelination in Experimental Autoimmune Encephalomyelitis and Cuprizone Models. To verify the role of astrocyte TrkB in demyelination, we evaluated myelin in the spinal cord white matter of adult GFAPTrkB knockout (KO) mice, which lack TrkB in GFAP-positive cells (7), and wild-type (TrkB WT) littermates under normal physiological conditions and during experimental autoimmune encephalomyelitis (EAE). Immunohistochemistry experiments demonstrated that MBP expression in the spinal cord of naïve GFAPTrkB KO mice was comparable to that of control animals, indicating that the absence of astrocyte TrkB per se does not affect physiological myelination in the CNS (Fig. 2*B*). However, GFAPTrkB KO mice did not display the pronounced myelin loss evident in TrkB WT animals during experimental neuroinflammation (Fig. 2 *A* and *B*).

Considering that immune cell infiltration is reduced in GFAPTrkB KO EAE mice (7) and that protection from demyelination may thus result indirectly from the limited inflammatory load, we moved our attention to a nonimmune-mediated demyelination model induced by cuprizone (CPZ) diet. CPZ is a copper chelating agent, which induces gliosis and oligodendrocyte loss in distinct brain regions, including the corpus callosum (CC), when supplemented to normal rodent chow (11, 12). When compared with tissues from animals receiving a normal diet, demyelination in the CC of CPZ-fed TrkB WT mice appeared limited at 2 wk but was very pronounced after 4 wk on the diet (Fig. 2*C*). In the same animals, we checked the expression of TrkB-T1, the truncated TrkB isoform, which is commonly expressed in glia cells during development or after injury (7, 13, 14). While absent in the CC of the normal diet group, TrkB-T1 was strongly induced by the CPZ diet and was already visible at 2 wk (Fig. 2*D*). Quantification of TrkB-T1 and MBP signals in these groups of animals underlined the inverse relationship between TrkB-T1 expression and MBP content (Fig. 2*E*). Double immunofluorescence followed by confocal imaging demonstrated that astrogliosis induced by the CPZ diet was associated with TrkB-T1 up-regulation (Fig. 2 *F*, *Right* and Fig. 2*G*).

To verify whether demyelination depended on astrocyte TrkB, we fed GFAPTrkB KO mice and control WT littermates with CPZ or a normal diet and analyzed TrkB and myelin expression in the CC of these animals. TrkB mRNA levels increased significantly with the CPZ diet in TrkB WT animals, but not in the GFAPTrkB KO mice (*SI Appendix*, Fig. S2 *A* and *B*). GFAPTrkB

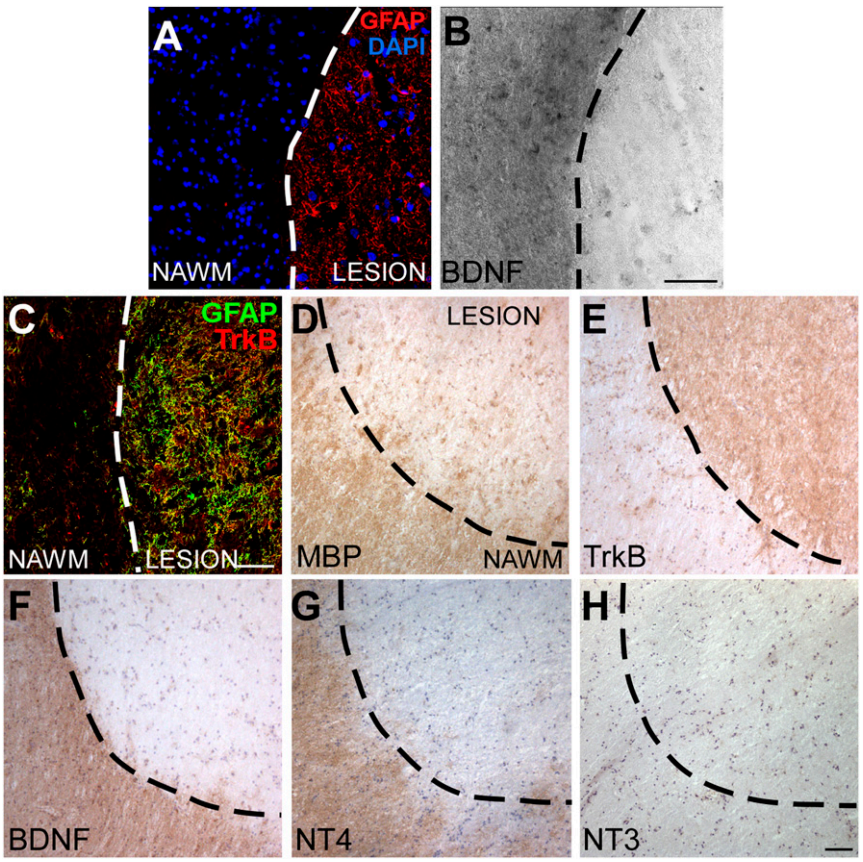

Fig. 1. TrkB ligands are not expressed in human MS lesions. (*A* and *B*) Representative immunofluorescence staining for GFAP (*A*) combined with in situ hybridization for BDNF mRNA (*B*) on human MS white matter. (*C*) Double immunofluorescence stainings for GFAP (green) and TrkB (red) in an MS lesion and nearby NAWM. (*D–H*) Immunohistochemistry for MBP, TrkB, BDNF, NT4, and NT3 on serial sections of a human chronic inactive MS lesion. Representative images of five analyzed MS lesions from five different subjects are shown. Dashed line demarcates lesion border. (Scale bars: 50 μm in *A–C*, 100 μm in *D–H*.)

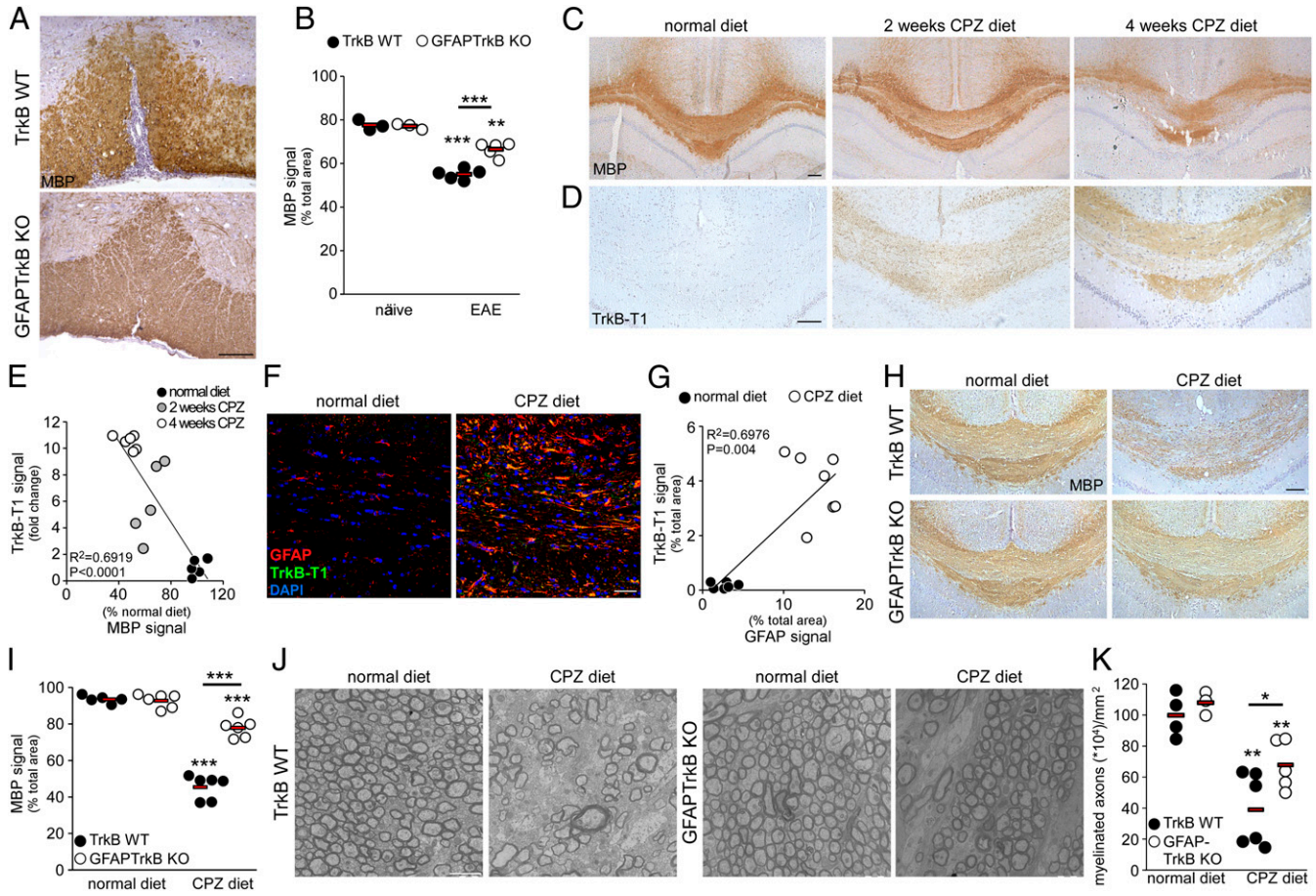

Fig. 2. TrkB expression in astrocytes supports demyelination in EAE and cuprizone models. (*A*) Representative immunohistochemistry stainings for myelin basic protein (MBP) in the spinal cord white matter of TrkB WT and GFAPTrkB KO mice during EAE. (*B*) Quantification of MBP signal in the spinal cord of naïve or EAE TrkB WT and GFAPTrkB KO animals derived from two independent EAE experiments. (*C* and *D*) Representative immunohistochemistry stainings for MBP (*C*) and TrkB-T1 (*D*) in the CC of TrkB WT animals fed with normal chow after 2 or 4 wk of CPZ diet. (*E*) Inverse correlation between TrkB-T1 expression and MBP signal during CPZ diet ($n = 5$ to 6 mice/group). (*F*) Representative double immunofluorescence stainings for GFAP (red) and TrkB-T1 (green) in the CC of normal diet (*Left*) or CPZ-treated (*Right*) TrkB WT mice. DAPI was used for nuclear staining. (*G*) Correlation between TrkB-T1 and GFAP expression in TrkB WT mice ($n = 6$ to 7 mice/group). (*H* and *I*) Representative immunohistochemistry stainings depicting MBP loss mainly in TrkB WT animals during CPZ diet (*H*, *Upper*) and not in GFAPTrkB KO mice (*H*, *Lower*) and relative quantification (*I*) ($n = 5$ to 6 mice/group derived from two independent experiments). (*J* and *K*) Electron microscopy images of the CC of TrkB WT or GFAPTrkB KO animals (*J*, $n = 3$ to 6 mice/group) during normal or CPZ diet and quantification of myelinated axons (*K*). Asterisks indicate statistical significance between conditions of the same genotype. Asterisks above bar indicate statistical significance between different genotypes.***$P < 0.001$, **$P < 0.01$, *$P < 0.05$. In *B*, *E*, *G*, *I*, and *K*, each dot represents a single animal; red bars represent means of the values. (Scale bars: 100 μm in *A*, *C*, *D*, and *H*; 30 μm in *F*; 2 μm in *J*.)

KO mice showed normal MBP levels and tissue ultrastructure when fed with a normal diet (Fig. 2 *H*–*K*). MBP content decreased by 25% and 50% in control mice after 2 or 4 wk on the CPZ diet, respectively (*SI Appendix*, Fig. S3 and Fig. 2 *H* and *I*), while it was relatively preserved in CPZ-fed GFAPTrkB KO mice (*SI Appendix*, Fig. S3 and Fig. 2 *H* and *I*). Ultrastructure examination confirmed severe loss of myelinated axons in TrkB WT mice on the CPZ diet, whereas the loss was less pronounced in transgenic animals (Fig. 2 *J* and *K*).

Overall, the in vivo evidence indicated a relevant role for astrocyte TrkB in white matter demyelination.

Astrocyte Responses to Neurotrophins Do Not Affect Myelin-Forming Cells. To verify whether astrocyte activation via TrkB may directly affect the biology of myelin-forming cells, we developed an in vitro model where rat primary oligodendrocytes (OLs) or their precursor cells (OPCs) were exposed to conditioned media from mouse primary astrocytes stimulated with the TrkB ligand BDNF or the typical inflammatory cytokine IL1. After an 8-h stimulation, media were changed to remove recombinant factors, and astrocyte-conditioned media (ACM) were collected after an additional 24-h culture. Under these conditions, astrocytes release NO in response to TrkB ligands, thus inducing neuronal death (7). As expected, ACM from BDNF- or IL1-stimulated cells triggered degeneration of primary spinal neurons (*SI Appendix*, Fig. S4 *A*–*C*). However, addition of the same ACM to myelin forming cells did not exert any effect. In fact, ACM did not affect survival and proliferation of OPCs (positive for O4 staining) (*SI Appendix*, Fig. S4 *D*–*F*), and altered neither OPC differentiation into mature MBP-positive OLs (*SI Appendix*, Fig. S4 *G*–*J*) nor the state of mature OLs (*SI Appendix*, Fig. S4 *K*–*M*). Overall, these experiments demonstrated that the toxic astrocyte TrkB-dependent mechanism driving neurodegeneration in response to neurotrophins was not implicated in oligodendrocyte damage.

TrkB Supports Astrocyte Functions Necessary for Scar Formation. To explore the role of TrkB in astrocyte function during neuroinflammation, we analyzed in vitro activation, migration, and proliferation of primary astrocytes from GFAPTrkB KO and TrkB WT mice.

First, we evaluated nuclear translocation of the inflammatory transcription factor NF-κB on exposure to BDNF or IL1. As shown in Fig. 3*A*, nuclei became positive for NF-κB in response to BDNF in TrkB WT cultures but not in GFAPTrkB KO astrocytes (Fig. 3 *A* and *B*), demonstrating a clear involvement of TrkB in the activation of inflammatory responses in response to neurotrophins. On the other hand, IL1 equally induced NF-κB translocation in TrkB WT and KO cultures (Fig. 3 *A* and *B*), indicating that TrkB-deficient astrocytes maintained the inflammatory potential in response to stimuli other than BDNF. This is in accordance with published data showing that NO, the production of which is NF-κB dependent, is similar in TrkB WT and KO cultures in response to IL1 (7). However, while gliosis and nitrosative stress (detected as GFAP and nitrotyrosine signal, respectively) were strongly enhanced in the CC of TrkB WT mice after CPZ diet, significantly these events were greatly reduced in GFAPTrkB KO mice (Fig. 3 *C*–*F*), indicating that astrocyte TrkB was necessary for scar formation in vivo.

Generation of the gliotic scar after injury requires the migration and proliferation of the astrocytes (1). Interestingly, when challenged in a scratch assay, which mimics damage in vitro, the GFAPTrkB KO astrocytes filled the gaps more slowly and less efficiently than control WT cells (Fig. 3 *G* and *H*). Further, when assessing in vitro proliferation, no difference in basal growth emerged between TrkB WT and KO astrocytes (Fig. 3*I*). However, exposure to BDNF for 7 d significantly boosted the proliferative response of WT astrocyte but not that of TrkB-deficient cells (Fig. 3*J*). Importantly, we observed the same impaired proliferative responses in GFAPTrkB KO astrocytes when cells were exposed to IL1 or CPZ (Fig. 3*J*), indicating that TrkB signaling also supported proliferative adaptation of the astrocyte to inflammatory or toxic mediators.

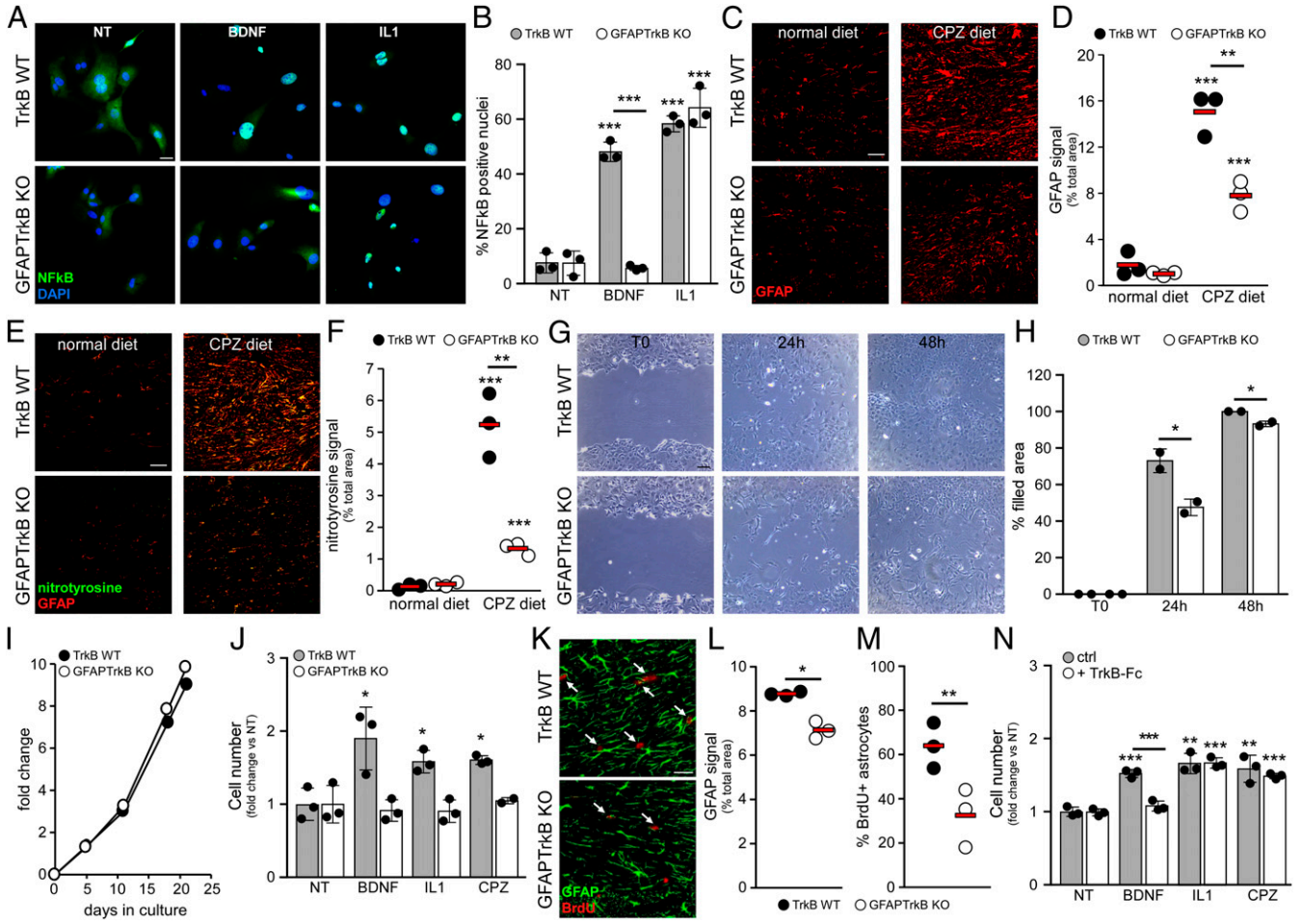

Fig. 3. TrkB supports astrocyte functions necessary for scar formation. (*A* and *B*) Representative immunofluorescence staining (*A*) and quantification (*B*) for NF-κB in cultured TrkB WT (*A*, *Upper*) and GFAPTrkB KO (*A*, *Lower*) astrocytes (NT, not treated, or stimulated with BDNF or IL1). Cells were counterstained with DAPI. (*C* and *D*) Representative immunofluorescence staining for GFAP immunoreactivity (*C*) in the CC of CPZ-treated animals compared with normal diet mice ($n = 3$ mice/group) and relative quantification (*D*). (*E* and *F*) Double immunofluorescence stainings for GFAP (*E*, red) and nitrotyrosine (*E*, green) in the CC of TrkB WT and GFAPTrkB KO animals fed with normal or CPZ diet and (*F*) quantification of nitrotyrosine signal ($n = 3$ mice/group). (*G* and *H*) Representative phase contrast images (*G*) of TrkB WT and KO astrocyte cultures during the scratch assay and relative quantification (*H*). (*I*) Basal proliferation rate of TrkB WT and KO astrocyte cultures. (*J*) Proliferation of TrkB WT and KO astrocytes after exposure to BDNF, IL1, or CPZ for 7 d. (*K*–*M*) Double immunofluorescence stainings for GFAP (green) and BrdU (red) in the CC of TrkB WT and GFAPTrkB KO mice after 1 wk of the CPZ diet, and relative quantifications (*L* and *M*) ($n = 3$ mice/group). Arrows in *K* highlight BrdU$^+$ astrocytes. (*N*) TrkB WT astrocyte proliferation after exposure to BDNF, IL1, or CPZ for 7 d in the presence or absence of TrkB-Fc protein. In *J* and *N*, basal proliferation (NT) after 7 d was normalized to day 0, and stimulated proliferation was expressed as fold change relative to NT. Asterisks indicate statistical significance between conditions of the same genotype. Asterisks above the bar indicate statistical significance between different genotypes. ***$P < 0.001$, **$P < 0.01$, *$P < 0.05$. In *D*, *F*, *L*, and *M*, each dot represents a single animal; red bars represent means. In *B*, *H*, *J*, and *N*, data are presented as mean ± SD. Representative data of one out of two to four independent experiments are shown. (Scale bars: 30 μm in *A*, *C*, *E*, and *K*; 100 μm in *G*.)

To verify whether TrkB had an impact on the initial proliferative responses of the astrocyte in vivo, we administered BrdU during the CPZ diet and killed the animals after 1 wk of the diet. Though GFAP signal in the CC of control mice was still modest at this early timepoint, it was already lower in CC from GFAPTrkB KO animals (Fig. 3 *K* and *L*). Further, the frequency of proliferating astrocytes was almost halved in GFAPTrkB KO mice compared with control mice (Fig. 3 *K* and *M*), thus demonstrating that TrkB signaling supported astrocyte proliferation in vivo.

To assess the potential involvement of endogenously produced neurotrophins in IL1- or CPZ-induced proliferation in vitro, we cultured TrkB WT astrocytes in the presence of soluble TrkB-Fc receptor. As expected, addition of TrkB-Fc blocked BDNF-induced proliferation (Fig. 3*N*). Importantly, it did not hamper IL1- or CPZ-induced proliferation, demonstrating that the proliferation boost triggered by these stimuli did not depend on endogenously produced neurotrophins (Fig. 3*N*).

In conclusion, these results indicated that independently of specific ligand binding, TrkB fostered astrocyte migration and proliferation in response to inflammatory or toxic insults.

Astrocytes Up-Regulate Copper Transporters during Human and Experimental Neuroinflammation. Since copper can be chelated by CPZ and alterations in copper levels may affect CNS function (15, 16), we initially investigated copper levels by inductively coupled plasma atomic emission spectrometry (ICP-AES) of sera from healthy controls and MS subjects. As shown in Fig. 4*A*, total serum copper differed among sexes, with higher levels in healthy or MS females than in males. However, no difference in serum copper concentration emerged between healthy and MS subjects after sex stratification (Fig. 4*A*), indicating that MS was not characterized by dysregulation of peripheral copper levels.

Copper trafficking in the CNS is primarily regulated at barriers including the BBB, where endothelial cells take copper up from the blood and direct it into the parenchyma (17). Cellular copper

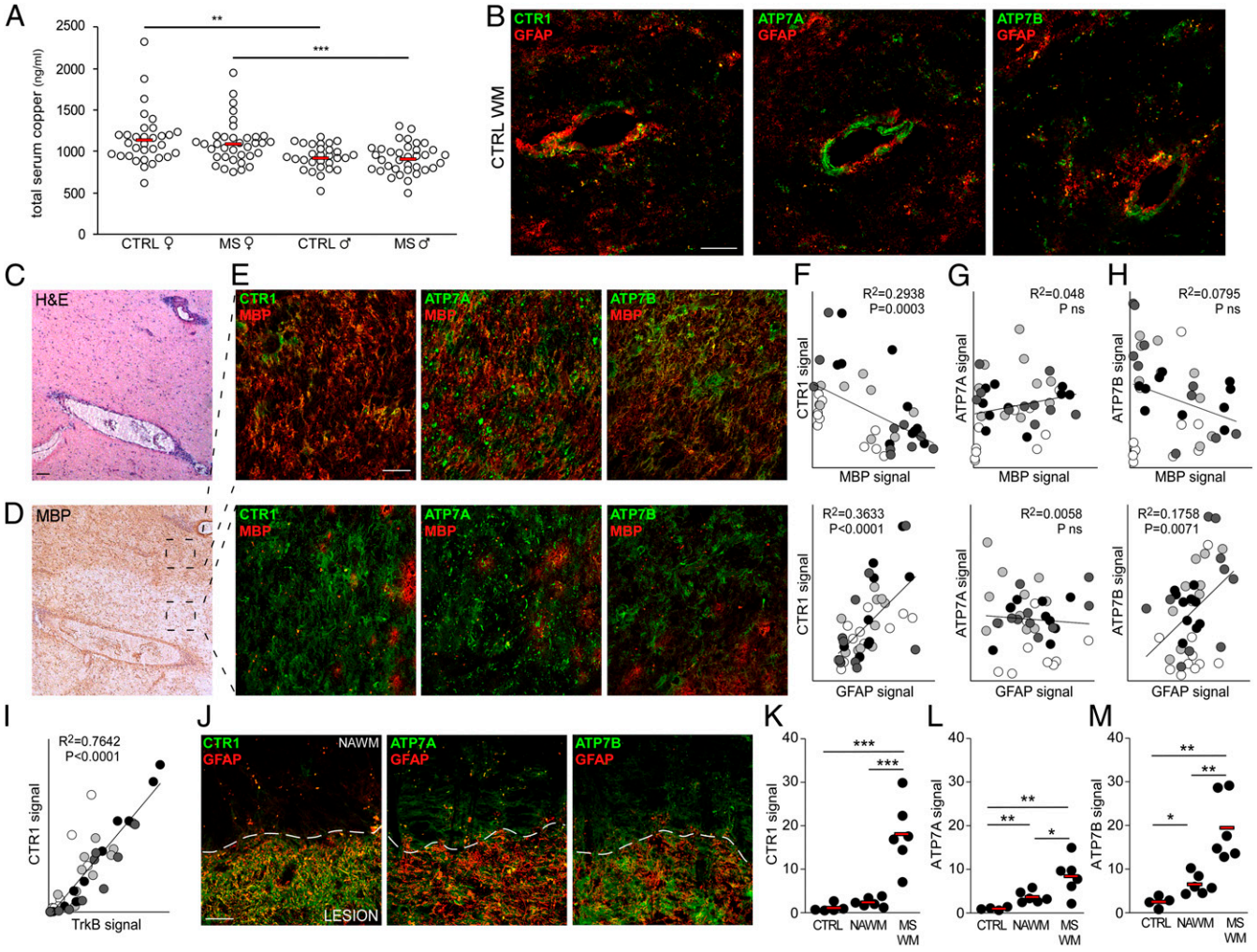

Fig. 4. Copper transporters are up-regulated in MS white matter. (*A*) Total copper content in the sera of healthy or MS subjects stratified by sex (CTRL female $n = 32$; MS female $n = 35$; CTRL male $n = 29$; MS male $n = 35$). (*B*) Representative double immunofluorescence stainings for GFAP (red) and CTR1/ATP7A/ATP7B (green) in one CTRL white matter (out of four analyzed). (*C* and *D*) Representative hematoxylin-eosin (H&E) and MBP stainings of an active MS lesion (out of four analyzed). (*E*) Representative double immunofluorescence stainings for MBP (red) and CTR1/ATP7A/ATP7B (green) in areas of an active MS lesion variable for MBP levels (out of four analyzed). (*F–I*) Correlation between MBP (*Upper*) or GFAP (*Lower*) and CTR1 (*F*)/ATP7A (*G*)/ATP7B (*H*) and between CTR1 and TrkB (*I*) in active MS lesions. Each color indicates a single lesion ($n = 4$) and each dot represents a single quantified image. (*J*) Representative double immunofluorescence stainings for GFAP (red) and CTR1/ATP7A/ATP7B (green) of a chronic inactive MS lesion (out of six analyzed). (*K–M*) Quantification of CTR1 (*K*), ATP7A (*L*), and ATP7B (*M*) signals in CTRL WM, NAWM, and chronic inactive MS WM plaques. Each dot represents a single sample ($n = 5$ to 6). In *F–I* and *K–M*, protein signals are reported as percentage of total area. ***$P < 0.001$, **$P < 0.01$, *$P < 0.05$. In *A* and *K–M*, red bars represent means. (Scale bars: 50 μm in *B*, *E*, and *J*; 100 μm in *C* and *D*.)

uptake is specifically mediated by Cu transporter 1 (CTR1), while copper efflux, necessary in case of metal overload, involves two ATPases, ATP7A and ATP7B (17). CTR1, ATP7A, and ATP7B were mainly localized at the vascular/perivascular level in human normal control white matter (Fig. 4*B*).

In active MS lesions, characterized by immune cell infiltration and variable MBP levels (Fig. 4 *C* and *D*), copper transporters were up-regulated (Fig. 4 *E–H*). Signal quantification in distinct areas of active MS lesions highlighted an inverse correlation between CTR1 expression and myelin content and a direct correlation between CTR1 or ATP7B and astrogliosis (Fig. 4 *F–H*) and between CTR1 and TrkB (Fig. 4*I*). Similarly, fully demyelinated chronic inactive MS lesions were characterized by the up-regulation of all copper transporters, with higher levels for CTR1 and ATP7B (Fig. 4 *J–M*), mainly on GFAP-positive astrocytes (Fig. 4*J*). Interestingly, while ATP7A and ATP7B were also slightly augmented in NAWM surrounding the demyelinated lesion (Fig. 4 *J*, *L*, and *M*), CTR1 signal perfectly demarcated the glial scar (Fig. 4 *J* and *K*), similarly to TrkB staining (*SI Appendix*, Fig. S5).

Copper levels in the spinal cord of perfused EAE and control animals were comparable (Fig. 5*A*), thus excluding gross copper accumulation during neuroinflammation. Analogously to the human CNS, CTR1, ATP7A, and ATP7B were weakly expressed in spinal cord (Fig. 5*B*) and CC (Fig. 5*D*) of control mice, while intensely augmented on astrocytes during EAE (Fig. 5*C*) or after the CPZ diet (Fig. 5 *E* and *G–I*). Importantly, CTR1 and ATP7A up-regulation induced by the CPZ diet did not occur in GFAPTrkB KO mice (Fig. 5 *F* and *G–H*), while ATP7B levels remained high in the transgenic animals fed with CPZ (Fig. 5 *F* and *I*), indicating astrocyte TrkB-dependent induction of CTR1 and ATP7A.

CTR1 Up-Regulation Is Dependent on Astrocyte TrkB. Since CTR1 up-regulation in vivo was TrkB dependent and correlated with demyelination in human MS active and chronic lesions, we further investigated the role of TrkB in the first step of copper trafficking, i.e., copper uptake via CTR1 in glial cells. While basal CTR1 mRNA levels in cultured astrocytes from GFAPTrkB KO and TrkB WT mice were similar (*SI Appendix*, Fig. S6*A*), CTR1 protein expression was much lower in TrkB-deficient astrocytes compared with WT cells (Fig. 6*A*). IL1 transiently up-regulated CTR1 mRNA in WT cells (*SI Appendix*, Fig. S6*B*). Importantly, exposure to 100 ng/mL copper (the free copper concentration in normal human serum) (18) or to inflammatory/toxic mediators

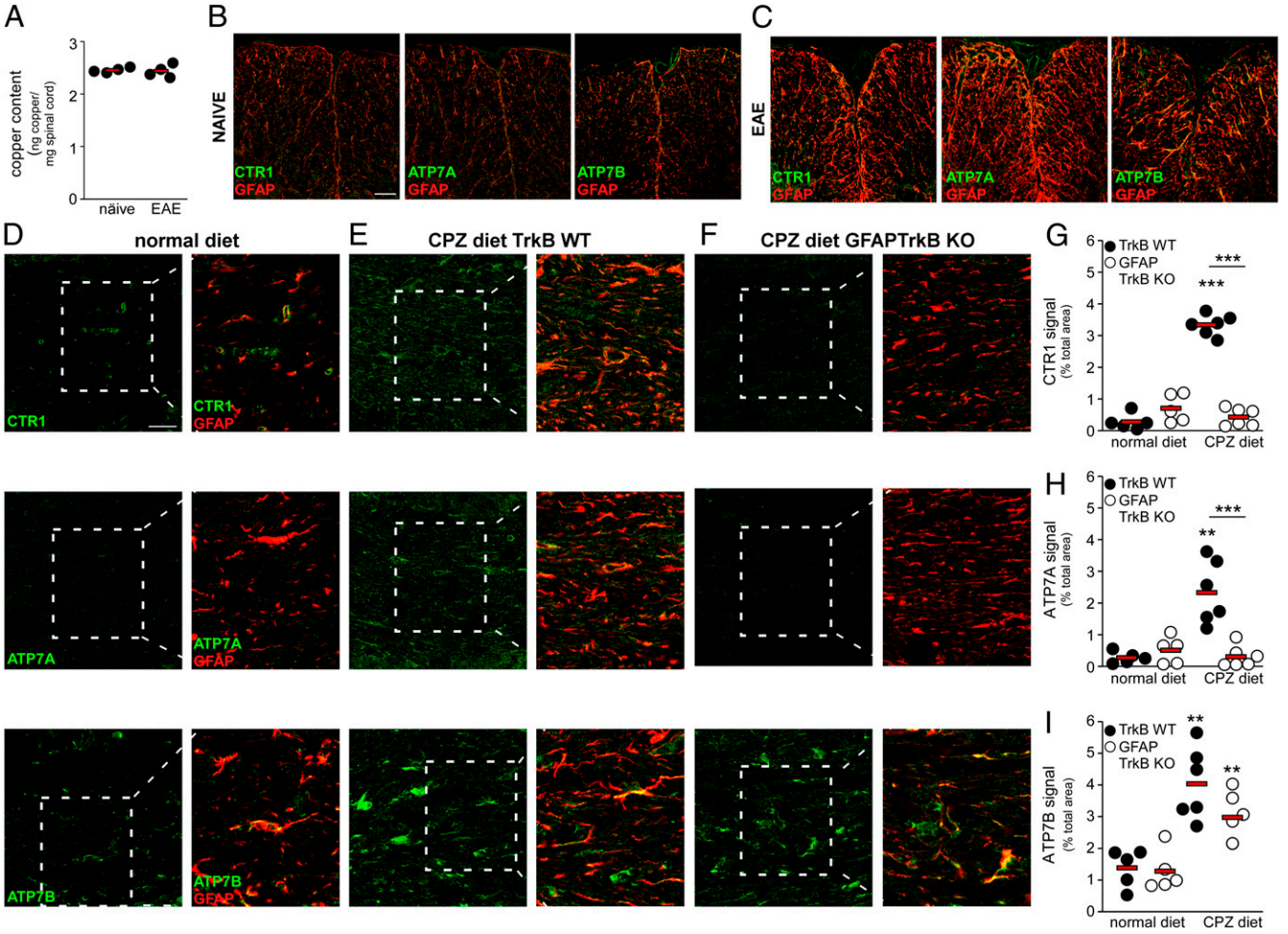

Fig. 5. Astrocytes up-regulate copper transporters during neuroinflammation in experimental MS depending on TrkB expression. (*A*) Total copper content in the spinal cord of naïve and EAE mice measured by inductively coupled plasma atomic emission spectrometry ($n = 4$ mice/group). (*B* and *C*) Double immunofluorescence stainings for GFAP (red) and CTR1/ATP7A/ATP7B (green) in naïve (*B*) and EAE (*C*) spinal cord. (*D–I*) Representative stainings (*D–F*) for GFAP (red) and CTR1/ATP7A/ATP7B (green) in the CC from TrkB WT or GFAPTrkB KO mice ($n = 5$ to 6 mice/group derived from two independent experiments) on normal or CPZ diets and (*G–I*) relative quantifications. Magnifications are shown in *Insets*. In *G–I*, asterisks indicate statistical significance between conditions from the same genotype. Asterisks above the bar indicate statistical significance between different genotypes. ***$P < 0.001$, **$P < 0.01$. In *A* and *G–I* each dot represents a single animal; red bars represent means. (Scale bars: 50 μm in *B–C*; 30 μm in *D–F*.)

(IL1 or CPZ) increased CTR1 mRNA (*SI Appendix*, Fig. S6*C*) and protein levels (Fig. 6 *B* and *C*) in TrkB WT astrocytes but not in GFAPTrkB KO cells. These observations indicate that TrkB signaling operated downstream injury signals, including those for copper, and directly supported CTR1 up-regulation in glia cells.

Although lacking a catalytic tyrosine kinase domain, astrocyte TrkB induces intracellular calcium flux in response to BDNF (13). Calcium imaging experiments confirmed that BDNF evoked Ca^{2+} waves in TrkB WT and not KO astrocytes (Fig. 6*E*). Interestingly, copper, IL1, and CPZ also activated intracellular Ca^{2+} fluxes in a TrkB-dependent process, as KO cells failed to generate calcium flux in response to any of these stimuli (Fig. 6 *D* and *E*). To verify whether activation of calcium waves was necessary for the modulation of CTR1 expression, we blocked intracellular calcium flux with thapsigargin (TG), an inhibitor of endoplasmic Ca^{2+} ATPase, in control or stimulated WT astrocytes. Remarkably, TG blocked CTR1 mRNA (*SI Appendix*, Fig. S6*D*) and protein up-regulation (Fig. 6 *F* and *G*) in response to copper, IL1, or CPZ, demonstrating that control of Ca^{2+} flux via TrkB is indispensable for copper uptake by astrocytes.

In addition to CTR1, primary mouse astrocytes displayed the ATPases ATP7A and ATP7B on the cell membrane (*SI Appendix*, Fig. S6*E*), indicating that these cells may also redistribute copper. In conventional culture conditions, copper derives from serum added to the media and is low due to serum dilution. In fact, copper levels in astrocyte-conditioned media were negligible (Fig. 6*H*), even when cells were stimulated with IL1 to up-regulate copper uptake via CTR1. However, if after IL1 exposure WT astrocytes were briefly incubated with high copper levels for 4 h and then washed and exposed to normal culture medium, their ACM contained copper after 24 h (Fig. 6*H*). Notably, TrkB KO cells released a much lower amount of copper than control astrocytes (Fig. 6*H*).

Finally, addition of copper to mature oligodendrocyte cultures reduced structural complexity (*SI Appendix*, Fig. S7 *A–C*) and induced oligodendrocyte (Fig. 6 *I* and *J*) and myelin loss (Fig. 6 *I*, K, and L) if given at the concentration of free copper in human sera (100 ng/mL), indicating that serum-free copper levels can trigger demyelination. This observation was replicated with ACM from TrkB WT astrocytes exposed to copper and diluted to have 100 ng/mL of free copper. In fact, OLs' exposure to copper-enriched ACM from TrkB WT astrocytes resulted in OL and myelin loss (Fig. 6 *M–P* and *SI Appendix*, Fig. S7 *D–F*), while proportionally diluted ACM from GFAPTrkB KO cells did not promote OLs' death (Fig. 6 *N–P* and *SI Appendix*, Fig. S7 *E* and *F*). Toxicity of copper-enriched ACM from WT astrocytes was inhibited by addition of the membrane-impermeable copper chelating agent bathocuproinedisulfonic acid disodium salt (BCS) (Fig. 6 *M–P* and *SI Appendix*, Fig. S7 *D–F*).

Overall, these data demonstrated that TrkB supported expression of copper transporters via modulation of glial calcium flux, thus leading to copper uptake and release, which in turn caused myelin and oligodendrocyte loss.

Discussion

In this study we provide evidence about alterations in copper transport in white matter lesions in MS and experimental MS in a process that depends on astrocytes. More specifically, the signaling mediated by the TrkB receptor in astrocytes responds to copper as well as inflammatory mediators, and thereby sustains the intracellular calcium flux necessary for the up-regulation of copper transporters. In this way, the astrocyte takes up and distributes copper in brain and spinal cord tissue, thus fostering demyelination and oligodendrocyte loss.

Astrocyte TrkB Fosters Scar Formation and White Matter Demyelination in the Absence of Neurotrophins. While expressed on a minor proportion of astrocytes under normal physiological conditions, TrkB is strongly elevated in neuroinflammatory conditions (7, 19). Here we show that myelin loss correlates with high TrkB expression in human and mouse white matter lesions, suggesting a connection between TrkB up-regulation on astrocytes and demyelinating processes during neuroinflammation.

Immunohistochemistry and electron microscopy experiments in naïve GFAPTrkB and control mice demonstrate that the absence of astrocyte TrkB per se does not affect physiological CNS myelination. Surprisingly, while mice lacking oligodendrocyte TrkB display unaltered (20) or exacerbated (21) demyelination upon CPZ diet compared with controls, transgenic mice lacking astrocyte TrkB are protected from demyelination induced by myelin-reactive T cell responses or toxic insults.

Considering that the TrkB-mediated astrocyte response to neurotrophins results in nitric oxide production (7) and that NO and peroxynitrite products may mediate oligodendrocyte injury (22, 23), we postulated a role for astrocyte TrkB in myelin loss via NO. However, this hypothesis was not corroborated by in vitro observations on myelin-forming cells exposed to astrocyte-conditioned media. Notably, protection from CPZ-induced demyelination in GFAPTrkB KO mice was associated with reduction in scar formation and nitrosative stress, suggesting an impairment in the inflammatory activation of the astrocyte. However, this possibility was excluded as TrkB KO astrocytes retain the potential to activate NF-κB (as shown in this study) and release NO (7) in response to inflammatory mediators.

TrkB-T1, the truncated TrkB isoform expressed by astrocytes (7, 24), may mediate cytoskeletal rearrangements via interaction with GDI1 (GDP dissociation inhibitor of Rho G proteins) thus inhibiting Rho GTPases activity (14, 25), and thereby regulating astrocyte morphogenesis, migration, and proliferation (19, 26). Indeed, we noticed that TrkB-deficient astrocytes were less efficient in migration and lost the ability to boost proliferation in response to stimuli distinct from BDNF. TrkB transactivation independent from neurotrophin binding has been described for neuronal full-length TrkB after exposure to estrogens (27), epidermal growth factor (28), G protein-coupled receptor ligands (29), some metals (30), or antidepressant drugs (31). Surprisingly, in our experiments glial proliferation depended on TrkB signaling but not on TrkB ligand binding, thus providing the evidence on glial TrkB-T1 transactivation downstream of inflammatory and CPZ signaling. CPZ administration represents a widely used strategy to induce CNS demyelination in vivo; however, it is unclear whether CPZ inactivates copper, induces directly OL death, and/or targets primarily the oligodendrocyte. Data from the literature indicate that CPZ–copper complexes may be still active (32), and cuprizone alone does not induce oligodendrocyte death in vitro (refs. 33, 34, and our study) unless concentrations in the millimolar range are used (34), and that astrocyte activation precedes demyelination in the CPZ model (35). In addition, our study shows that astrocyte proliferation is an in vivo and in vitro response to CPZ, which depends on TrkB. Importantly, BDNF wanes in the corpus callosum on a cuprizone diet (36) and, as shown in our study, in human MS chronic inactive lesions, which also lack the expression of NT-3 and NT-4, thus confirming the scenario that alternative cues sustain TrkB signaling in reactive astrocytes and, possibly, lead to demyelination.

Enhanced Copper Transport in the CNS Tissue via Astrocyte TrkB Mediates Demyelination. Our neuropathological observations indicate robust dysregulation of copper transport in human and experimental MS. Copper is essential for normal CNS physiology as it serves as a cofactor for proteins involved in energy metabolism, antioxidative defense, and neurotransmitter and neuropeptide synthesis (15). Moreover, evidence of copper accumulation in synaptic vesicles suggests a potential neuromodulatory function of this metal (37). Copper is absorbed in the gut from the diet, transported to the liver, and released into the bloodstream. Due to

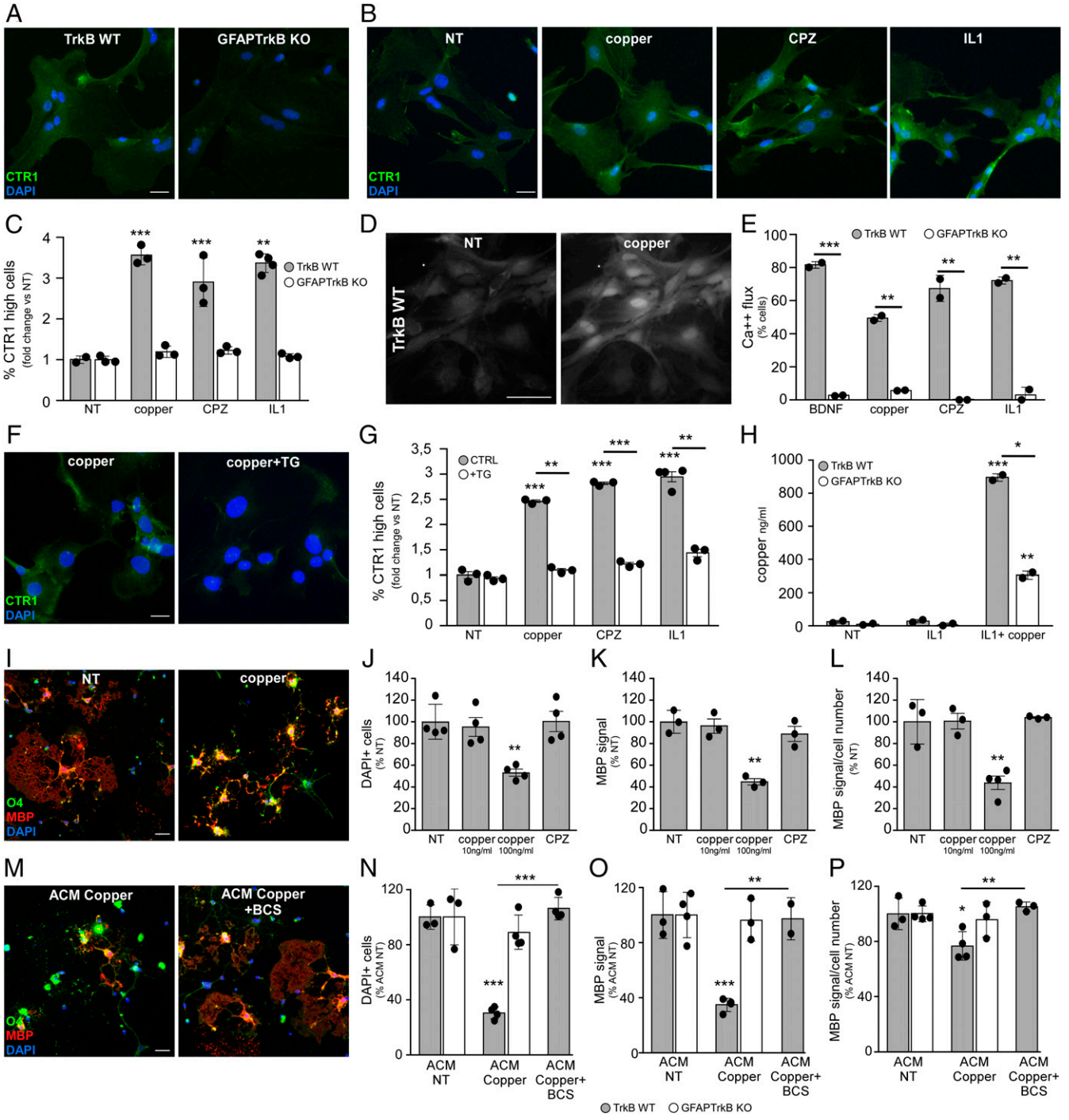

Fig. 6. CTR1 up-regulation depends on astrocyte TrkB. (*A*) CTR1 staining in TrkB WT and GFAPTrkB KO astrocyte cultures. (*B* and *C*) CTR1 signal in nontreated (NT) or stimulated TrkB WT and GFAPTrkB KO astrocyte cultures (*B*) and relative quantifications (*C*). (*D* and *E*) Fluo-4 signal in untreated or copper-treated astrocytes (*D*) and percentage of cells performing at least 1 Ca^{2+} oscillation under distinct in vitro conditions (*E*). (*F* and *G*) CTR1 staining in copper-stimulated astrocytes in the absence (*Left*) or presence (*Right*) of calcium inhibitor thapsigargin (TG) (*F*) and relative quantification (*G*). (*H*) Copper levels in ACM from nontreated or stimulated astrocytes measured by inductively coupled plasma atomic emission spectrometry. (*I*) Representative stainings for O4 (green) and MBP (red) in oligodendrocyte cultures NT or treated with 100 ng/mL copper. (*J–L*) Quantification of oligodendrocyte number (*J*), total MBP signal (*K*), and relative MBP signal per cell (*L*) in OL cultures under distinct conditions. Data are reported as percentage of NT condition. (*M*) Representative stainings for O4 (green) and MBP (red) in oligodendrocyte cultures exposed to ACM from copper-loaded TrkB WT astrocytes. Eventually, ACM added with copper chelator BCS was given. (*N–P*) Quantification of oligodendrocyte number (*N*), total MBP signal (*O*), and relative amount of MBP per cell (*P*) in OL cultures treated with ACM from TrkB WT and GFAPTrkB KO astrocytes. Data are reported as percentage of the corresponding ACM NT. Asterisks indicate statistical significance between conditions from the same genotype. Asterisks above the bar indicate statistical significance between genotypes. ***$P < 0.001$, **$P < 0.01$, *$P < 0.05$. In *A*, *B*, *F*, *I*, and *M*, DAPI was used for nuclear staining. In *C*, *E*, *G*, *J–L*, and *N–P*, data are presented as mean ± SD. Representative data of one out of two to four independent experiments in all cases but *E*, where the sum of two independent experiments is reported and error bars represent SEM. (Scale bars: 30 μm.)

the toxic potential and redox activity of free copper, this metal is mainly found in complexes with plasma proteins (17). A recent study reported higher copper concentration in MS sera and cerebral spinal fluid (CSF) than in control samples (38); however, this MS group had a major female component compared with the control group, underscoring potential sexual dimorphism for this measurement. Indeed, our biochemical quantification of total copper in healthy and MS sera indicated higher copper levels in women than in men but no difference between healthy and MS subjects in both sexes.

The small amount of free copper in the systemic circulation passes the blood brain barrier into the CNS parenchyma through specific membrane transporters expressed at the luminal side on endothelial cells. The copper transporter CTR1 is likely to be the major pathway for copper entry into CNS cells, while copper efflux, necessary in case of metal overload, is mediated by ATP7A and ATP7B (17). Exposure to excessive copper is highly toxic for neuronal cells (39, 40), thus copper homeostasis requires close control of transport, uptake, release, and storage.

We show that, while circulating copper levels are normal during disease, expression of copper transporters in the CNS is profoundly augmented during neuroinflammation, suggesting a rise in active uptake from the bloodstream and diffusion of the metal ions within CNS tissues. As a result of their strategic, close contact with the vasculature, astrocytes are the first CNS parenchymal cells that may encounter copper released by endothelial cells. In fact, cultured astrocytes are equipped with CTR1 (our study and ref. 41), are resistant against copper-induced toxicity (40–42), and thus may efficiently accumulate and release copper in a time- and concentration-dependent manner (our study and ref. 42). Importantly, astrocytes strongly up-regulate CTR1 during neuroinflammation in a TrkB- and calcium-dependent manner, as TrkB is necessary to support efficient glial calcium waves in response to copper and inflammatory mediators. As astrocytes exhibit high expression of copper exporters in human and experimental MS, the downstream effect may be copper redistribution to other cell types, thus leading to oligodendrocyte and myelin loss.

These findings shed light on the mechanisms governing both the active and the chronic states of demyelination in MS. The inverse correlation between myelin and CTR1 levels in active MS lesions suggests that structural and functional impairment of the BBB can cause serum copper entry into the CNS followed by astrocytic copper uptake and release and result in induction of demyelination. In chronic inactive MS lesions, though macroscopic BBB breakdown is less prominent, copper uptake and distribution may still be supported by the strong, persistent astrogliosis.

Copper and iron metabolism are closely interrelated, starting from the sharing of the cellular uptake transporter DMT1 to the role of copper as cofactor in proteins involved in iron homeostasis, such as ceruloplasmin, or as a modulator of the iron regulatory hormone hepcidin (16). Abnormal systemic copper levels may affect iron metabolism in the brain and, vice versa, iron levels influence CNS copper homeostasis (16). Our data indicating unchanged blood copper levels but up-regulated CNS copper transporters in MS patients do not support the hypothesis of systemic metal imbalance, but rather local transport dysregulation in the white matter lesions. While iron loss occurs in MS normal appearing white matter, iron deposits are observed at the edges of active and inactive demyelinated lesions (43). Whether these iron and copper imbalances are locally interconnected remains to be established.

Metal ion trafficking can be assessed in vivo by modern non-invasive imaging techniques, such as ^{64}Cu positron emission tomography. This method has already been used to visualize copper trafficking in brain tumors characterized by the up-regulation of copper transporters (44). We envisage that its application in MS can help to monitor local transport of the metal and lesion evolution in time and assess the impact of CNS-directed therapies on these copper-related pathological processes.

In conclusion, we speculate that copper transport via activated astrocytes exacerbates tissue injury and demyelination, and restoring normal copper homeostasis may be of importance for tissue repair. Whether reducing copper redistribution would be sufficient to halt lesion progression and therefore be a therapeutic target are highly relevant perspectives to be validated in future studies.

Materials and Methods

Details on human samples, animal models, generation of primary cell cultures, in vitro stimulations and assays, in situ hybridization, immunohistochemistry, electron microscopy, image analyses, copper measurements, flow cytometry, RNA extraction, real-time PCR, and statistics are provided in *SI Appendix, Materials and Methods*.

Data Availability. All study data are included in the article and/or *SI Appendix*.

ACKNOWLEDGMENTS. We thank all the clinicians at the neurology department of San Raffaele Scientific Institute for patient selection, personnel at Amici Centro Sclerosi Multipla for support with blood sampling, and all participants who donated blood for this study; Paola Podini at San Raffaele Scientific Institute for support with electron microscopy experiments; the Lab of Separative Techniques at San Raffaele Scientific Institute for copper measurements; and Michela Bartoccetti at the Immunobiology of Neurological Disorders Lab, San Raffaele Scientific Institute, for support during calcium imaging experiments. This work was funded by the Italian Ministry for Health, Fondazione Italiana Sclerosi Multipla (FISM) (Grants 2012/R/7 and 2016/R/14 to C.F.) and cofinanced with the 5 per mille public funding. E.C. was supported by a FISM research fellowship (Cod. 2013/B/3).

1. M. V. Sofroniew, Astrogliosis. *Cold Spring Harb. Perspect. Biol.* **7**, a020420 (2014).
2. I. Molina-Gonzalez, V. E. Miron, Astrocytes in myelination and remyelination. *Neurosci. Lett.* **713**, 134532 (2019).
3. E. Colombo, C. Farina, Astrocytes: Key regulators of neuroinflammation. *Trends Immunol.* **37**, 608–620 (2016).
4. H. Lassmann, Pathogenic mechanisms associated with different clinical courses of multiple sclerosis. *Front. Immunol.* **9**, 3116 (2019).
5. T. Zrzavy *et al.*, Loss of 'homeostatic' microglia and patterns of their activation in active multiple sclerosis. *Brain* **140**, 1900–1913 (2017).
6. S. Luchetti *et al.*, Progressive multiple sclerosis patients show substantial lesion activity that correlates with clinical disease severity and sex: A retrospective autopsy cohort analysis. *Acta Neuropathol.* **135**, 511–528 (2018).
7. E. Colombo *et al.*, Stimulation of the neurotrophin receptor TrkB on astrocytes drives nitric oxide production and neurodegeneration. *J. Exp. Med.* **209**, 521–535 (2012).
8. E. Colombo *et al.*, Fingolimod may support neuroprotection via blockade of astrocyte nitric oxide. *Ann. Neurol.* **76**, 325–337 (2014).
9. N. Miyamoto *et al.*, Astrocytes promote oligodendrogenesis after white matter damage via brain-derived neurotrophic factor. *J. Neurosci.* **35**, 14002–14008 (2015).
10. M. Kerschensteiner *et al.*, Activated human T cells, B cells, and monocytes produce brain-derived neurotrophic factor in vitro and in inflammatory brain lesions: A neuroprotective role of inflammation? *J. Exp. Med.* **189**, 865–870 (1999).
11. A. Zendedel, C. Beyer, M. Kipp, Cuprizone-induced demyelination as a tool to study remyelination and axonal protection. *J. Mol. Neurosci.* **51**, 567–572 (2013).
12. M. Kipp *et al.*, Experimental in vivo and in vitro models of multiple sclerosis: EAE and beyond. *Mult. Scler. Relat. Disord.* **1**, 15–28 (2012).
13. C. R. Rose *et al.*, Truncated TrkB-T1 mediates neurotrophin-evoked calcium signalling in glia cells. *Nature* **426**, 74–78 (2003).
14. K. Ohira *et al.*, A truncated tropomyosin-related kinase B receptor, T1, regulates glial cell morphology via Rho GDP dissociation inhibitor 1. *J. Neurosci.* **25**, 1343–1353 (2005).
15. I. F. Scheiber, J. F. Mercer, R. Dringen, Metabolism and functions of copper in brain. *Prog. Neurobiol.* **116**, 33–57 (2014).
16. T. Skjørringe, L. B. Møller, T. Moos, Impairment of interrelated iron- and copper homeostatic mechanisms in brain contributes to the pathogenesis of neurodegenerative disorders. *Front. Pharmacol.* **3**, 169 (2012).
17. W. Zheng, A. D. Monnot, Regulation of brain iron and copper homeostasis by brain barrier systems: Implication in neurodegenerative diseases. *Pharmacol. Ther.* **133**, 177–188 (2012).
18. G. A. McMillin, J. J. Travis, J. W. Hunt, Direct measurement of free copper in serum or plasma ultrafiltrate. *Am. J. Clin. Pathol.* **131**, 160–165 (2009).
19. J. J. Matyas *et al.*, Truncated TrkB.T1-mediated astrocyte dysfunction contributes to impaired motor function and neuropathic pain after spinal cord injury. *J. Neurosci.* **37**, 3956–3971 (2017).
20. J. L. Fletcher *et al.*, Targeting TrkB with a brain-derived neurotrophic factor mimetic promotes myelin repair in the brain. *J. Neurosci.* **38**, 7088–7099 (2018).

21. Y. Huang *et al*., Tropomyosin receptor kinase B expressed in oligodendrocyte lineage cells functions to promote myelin following a demyelinating lesion. *ASN Neuro* **12**, 1759091420957464 (2020).
22. C. Jack, J. Antel, W. Brück, T. Kuhlmann, Contrasting potential of nitric oxide and peroxynitrite to mediate oligodendrocyte injury in multiple sclerosis. *Glia* **55**, 926–934 (2007).
23. G. S. Scott, L. Virág, C. Szabó, D. C. Hooper, Peroxynitrite-induced oligodendrocyte toxicity is not dependent on poly(ADP-ribose) polymerase activation. *Glia* **41**, 105–116 (2003).
24. B. M. Fenner, Truncated TrkB: Beyond a dominant negative receptor. *Cytokine Growth Factor Rev.* **23**, 15–24 (2012).
25. K. Ohira *et al*., Truncated TrkB-T1 regulates the morphology of neocortical layer I astrocytes in adult rat brain slices. *Eur. J. Neurosci.* **25**, 406–416 (2007).
26. L. M. Holt *et al*., Astrocyte morphogenesis is dependent on BDNF signaling via astrocytic TrkB.T1. *eLife* **8**, e44667 (2019).
27. W. Wang *et al*., Estrogen's effects on excitatory synaptic transmission entail integrin and TrkB transactivation and depend upon beta1-integrin function. *Neuropsychopharmacology* **41**, 2723–2732 (2016).
28. D. Puehringer *et al*., EGF transactivation of Trk receptors regulates the migration of newborn cortical neurons. *Nat. Neurosci.* **16**, 407–415 (2013).
29. F. S. Lee, M. V. Chao, Activation of Trk neurotrophin receptors in the absence of neurotrophins. *Proc. Natl. Acad. Sci. U.S.A.* **98**, 3555–3560 (2001).
30. Y. Z. Huang, E. Pan, Z. Q. Xiong, J. O. McNamara, Zinc-mediated transactivation of TrkB potentiates the hippocampal mossy fiber-CA3 pyramid synapse. *Neuron* **57**, 546–558 (2008).
31. T. Rantamäki *et al*., Antidepressant drugs transactivate TrkB neurotrophin receptors in the adult rodent brain independently of BDNF and monoamine transporter blockade. *PLoS One* **6**, e20567 (2011).
32. N. Yamamoto, K. Kuwata, DFT studies on redox properties of copper-chelating cuprizone: Unusually high-valent copper(III) state. *J. Mol. Struct. Theochem.* **895**, 52–56 (2009).
33. L. A. Pasquini *et al*., The neurotoxic effect of cuprizone on oligodendrocytes depends on the presence of pro-inflammatory cytokines secreted by microglia. *Neurochem. Res.* **32**, 279–292 (2007).
34. A. Taraboletti *et al*., Cuprizone intoxication induces cell intrinsic alterations in oligodendrocyte metabolism independent of copper chelation. *Biochemistry* **56**, 1518–1528 (2017).
35. T. Tezuka *et al*., Cuprizone short-term exposure: Astrocytic IL-6 activation and behavioral changes relevant to psychosis. *Neurobiol. Dis.* **59**, 63–68 (2013).
36. M. W. VonDran, H. Singh, J. Z. Honeywell, C. F. Dreyfus, Levels of BDNF impact oligodendrocyte lineage cells following a cuprizone lesion. *J. Neurosci.* **31**, 14182–14190 (2011).
37. A. Hopt *et al*., Methods for studying synaptosomal copper release. *J. Neurosci. Methods* **128**, 159–172 (2003).
38. L. De Riccardis *et al*., Copper and ceruloplasmin dyshomeostasis in serum and cerebrospinal fluid of multiple sclerosis subjects. *Biochim. Biophys. Acta Mol. Basis Dis.* **1864** (5 Pt A), 1828–1838 (2018).
39. D. Marmolino, M. Manto, Pregabalin antagonizes copper-induced toxicity in the brain: In vitro and in vivo studies. *Neurosignals* **18**, 210–222 (2010).
40. P. V. Reddy, K. V. Rao, M. D. Norenberg, The mitochondrial permeability transition, and oxidative and nitrosative stress in the mechanism of copper toxicity in cultured neurons and astrocytes. *Lab. Invest.* **88**, 816–830 (2008).
41. I. F. Scheiber, J. F. Mercer, R. Dringen, Copper accumulation by cultured astrocytes. *Neurochem. Int.* **56**, 451–460 (2010).
42. I. F. Scheiber, M. M. Schmidt, R. Dringen, Copper export from cultured astrocytes. *Neurochem. Int.* **60**, 292–300 (2012).
43. S. Hametner *et al*., Iron and neurodegeneration in the multiple sclerosis brain. *Ann. Neurol.* **74**, 848–861 (2013).
44. P. Panichelli *et al*., Imaging of brain tumors with copper-64 chloride: Early experience and results. *Cancer Biother. Radiopharm.* **31**, 159–167 (2016).